E-Journal of Advanced Maintenance Vol.10 No.2 (2018) 1-8
Japan Society of Maintenology

A consideration on the use of shear waves to improve the sensitivity of an optical ultrasonic sensor for under-sodium viewers

Koichi SARUTA[1,3,*], Takuma SHIRAHAMA[2], Toshihiko YAMAGUCHI[3], and Masashi UEDA[3]

[1] *Applied Laser Research Group, Applied Laser and Innovative Technology Institute, Japan Atomic Energy Agency, 65-20 Kizaki, Tsuruga, Fukui 914-8585, Japan*
[2] *Tsuruga Office, NESI Inc., 2-1 Shiraki, Tsuruga, Fukui 919-1279, Japan*
[3] *Sodium Technology Development Group, Fast Reactor Plant Technology Development Department, Japan Atomic Energy Agency, 1 Shiraki, Tsuruga, Fukui 919-1279, Japan*

ABSTRACT

The present work is intended to investigate shear waves induced on stainless steel diaphragms by the incidence of ultrasonic waves, with the main emphasis on the understanding of the generation mechanism of the resultant second wave, in order to explore the possible use of the shear waves for improvement of the sensitivity of an optical ultrasonic sensor used for under-sodium viewers. The response of the diaphragms exposed to ultrasonic waves with different pressure profiles is measured by a heterodyne interferometer to examine the location where the shear waves are excited. The generation of the second wave is interpreted on the basis of interference of these shear waves. The effectiveness of the use of the shear waves is demonstrated by an improved sensitivity of 0.26 nm/kPa for a 3-mm-diameter and 5-μm-thick diaphragm. This sensitivity is approximately 7 times as high as the sensitivity achieved with the first wave, which is the displacement of the diaphragm caused by directly incident ultrasonic waves.

KEYWORDS

Optical ultrasonic sensor, Optical pressure sensor, Optical hydrophone, Under-sodium viewer, Fast reactor

ARTICLE INFORMATION

Article history:
Received 18 April 2018
Accepted 24 August 2018

1. Introduction

Ultrasonic imaging methods are well established and widely employed for non-destructive inspection and diagnosis in a variety of industries. For in-service inspection of a sodium-cooled fast reactor, several efforts have been made to develop an ultrasonic under-sodium viewer (USV) in order to perform visual inspection and maintenance of structural components in the reactor [1, 2]. Critical issues to design the imaging sensor array of USVs, which is built by arranging a number of ultrasonic sensors in a matrix form, include resolution, thermal resistance, and array size and weight. To provide a possible solution to these technical matters, the use of an optical ultrasonic sensor has been considered in place of using conventional piezoelectric transducers [3, 4].

This optical ultrasonic sensor consists of a diaphragm and a laser interferometer. The diaphragm is displaced by the pressure of incident ultrasonic waves, which is then measured by the laser interferometer. In this way the optical ultrasonic sensor measures the displacement corresponding to the pressure of ultrasonic waves. The diaphragm is one of the most important elements that govern the sensitivity of the optical ultrasonic sensor, which is defined as the ratio of the displacement to the pressure of ultrasonic waves, and in turn influences on the imaging quality of USVs. For a circular diaphragm with a radius r, thickness d, and modulus of elasticity E, the maximum deflection at the center of the diaphragm is proportional to r^4 and is inversely proportional to d^3 and E, under the assumption that static pressure is uniformly applied to the diaphragm [5]. Therefore, most of studies have been devoted to the development of thinner and flexible diaphragms using various materials in order to improve the sensitivity. For example, it has been reported that diaphragms made of silver,

*Corresponding author, E-mail: saruta.koichi@jaea.go.jp

silica, and graphene are capable of achieving high sensitivities of 1.6, 3.4, and 39.4 nm/kPa, respectively [6-8]. However, as far as diaphragms used for USVs are concerned, diaphragms need to be sufficiently robust and thick so as to resist the corrosive sodium coolant. Furthermore, it is necessary for the materials to satisfy the stringent safety requirements imposed on the nuclear power plant. All these restrictions must be taken into account in the development of a sensitive optical ultrasonic sensor for USVs.

In our previous study the sensitivity characteristics of stainless steel diaphragms, the material of which is commonly employed in a nuclear power plant, were examined with the thickness and diameter varied between 5 and 20 mm and between 3 and 10 mm, respectively [9]. We observed that two different waves with a time delay were induced on the diaphragm. The first wave resulted from the translational motion of the diaphragm, which concurred with the incidence of the ultrasonic wave, whereas the second wave was speculated to take place as a result of interference of shear waves that propagate over the diaphragm. The amplitude of both waves increased with decreasing diaphragm thickness. More importantly, however, the amplitude of the second wave became much larger than that of the first wave with decreasing diameter. Such diameter dependence was not observed for the first wave. This means that the use of the shear waves has a possibility to improve the sensitivity of the optical ultrasonic sensor, although few studies have focused on it and the characteristic of these shear waves are still incompletely understood. From our previous experimental results, little is known about the generation mechanism of the resultant second wave either.

In this paper we experimentally investigate the shear waves induced on stainless steel diaphragms, with the main emphasis on the understanding of the generation mechanism of the resultant second wave, in order to explore the possible use of the shear waves for improvement of the sensitivity of an optical ultrasonic sensor used for under-sodium viewers. The response of the diaphragms exposed to ultrasonic waves with different pressure profiles is measured by a heterodyne interferometer to examine the location where the shear waves are excited. The generation of the second wave is interpreted on the basis of interference of these shear waves. The effectiveness of the use of the shear waves is demonstrated by an improved sensitivity of 0.26 nm/kPa for a 3-mm-diameter and 5-mm-thick stainless steel diaphragm, which is approximately 7 times as high as the sensitivity achieved with the first wave.

2. Experimental setup

The diaphragms are fabricated by bonding a piece of 5-μm-thick foil on a 2-mm-thick substrate, both of which are made of stainless steel, by means of the thermal diffusion bonding technique. The substrate has circular apertures of 3, 5, and 10 mm in diameter, each one of which is sealed with the foil and thus acts as an independent diaphragm. Using the same material for the foil and substrate prevents the diaphragms from radially stretching or loosening owing to thermal expansion during the fabrication process.

The experimental setup for measuring the response of the diaphragms is shown in Fig. 1. The diaphragms are set on the sidewall of a water tank in such a way that the one side of the diaphragms has a contact with water, which is used in place of a sodium coolant in the present experiments, to receive ultrasonic waves emitted from a piezoelectric transducer (PZT). The transducer has a circular active element with a diameter of 5 mm, producing a narrow band ultrasonic burst wave with a center frequency of 5 MHz and a duration of ~1.5 μs. The pressure level and distribution exerted on each diaphragm are controlled by changing the distance between the diaphragm and the transducer with a linear translation stage. Actual pressure levels are measured with a needle hydrophone.

The waves induced on the diaphragms are measured by a heterodyne interferometer. The light source is an external cavity diode laser (ECDL), the wavelength of which is stabilized at 780 nm. The emitted light is divided into two beams with a polarizing beam splitter (PBS1): one for the reference and the other for the measurement. The reference beam is frequency shifted with an acousto-optic modulator (AOM). The measurement beam is coupled into a polarization maintaining fiber (PMF) so that the beam spot formed by a focusing lens (FL) can be scanned over each one of the diaphragms. The measurement beam reflected from the diaphragms is recombined with the reference beam by a

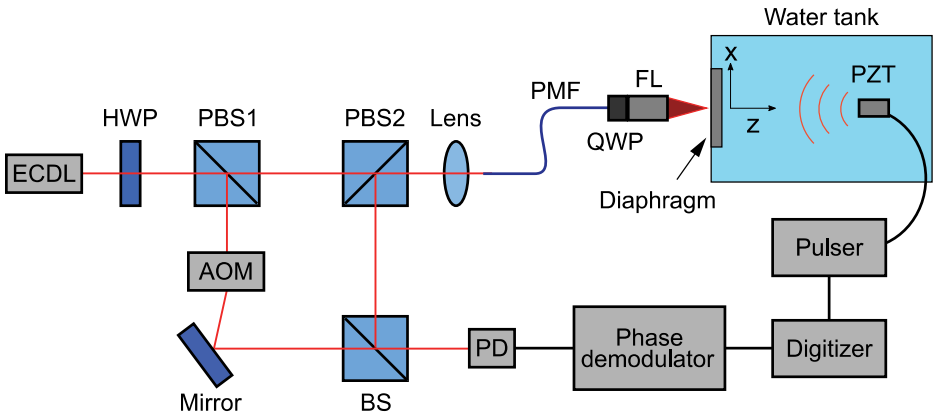

Fig. 1. Experimental setup for measuring the response of the diaphragms. ECDL, external cavity diode laser; HWP, half-wave plate; PBS, polarizing beam splitter; AOM, acousto-optic modulator; BS, beam splitter; PD, photodiode; PMF, polarization maintaining fiber; QWP, quarter-wave plate; FL, focusing lens; PZT, piezoelectric transducer.

beam splitter (BS), and the resultant interference signal is detected by a photodiode (PD). Demodulation of the interference signal is performed by a phase demodulator (PM) to retrieve the waveforms induced on the diaphragms.

3. Experimental results and discussion

Figure 2(a) shows the waveform of an ultrasonic wave measured by a needle hydrophone aligned to the center of the piezoelectric transducer. The observed waveform is typical of those from a 5-MHz narrow band piezoelectric transducer driven by a spike voltage from a pulser, comprised of several cycles of a 5-MHz wave with a decaying amplitude within a duration of ~1.5 μs. The pressure distribution of the ultrasonic wave observed in a plane normal to the propagation direction depends on the distance from the transducer. Figure 2(b) shows the one-dimensional positive pressure distributions taken by scanning the hydrophone along the x-axis with an interval of 0.25 mm in the plane, where the position at $x = 0$ is collinear with the center of the transducer. For clarity, a reduced number of measurement points (markers) are shown here. The profiles exhibit a Lorentzian-like shape. As the distance increases, the pressure distribution broadens with the central maximum dropping, approaching to a nearly uniform pressure level in the range of ±5.0 mm at $z = 250$ mm. It is worth noting that within the range of ±2.5 mm, the pressure monotonically decreases with increasing distance, whereas without that range, this monotonic relationship between the pressure and the distance does not hold. Comparing pressures at $x = \pm 5.0$ mm among the profiles, one can see that the pressure profile at $z = 150$ mm has the largest value, the pressure profile at $z = 50$ mm has the smallest value, and the rest profiles fall in between them. Although the pressure distribution was measured only on the horizontal axis, an axially symmetric profile around the central axis of the transducer may be assumed in the present experiments because of homogeneous and isotropic properties of water.

The response of the diaphragms was examined using the ultrasonic waves described above. Shown in Fig. 3 are several of the observed waveforms, which were taken by scanning the laser beam along the diameter on the 10-mm-diameter diaphragm from $x = 5.0$ mm to $x = -5.0$ mm at 0.5 mm increments. In these waveforms, time is referenced to the trigger signal generated by a pulser, and the time taken for the ultrasonic wave to travel the distance between the diaphragm and the transducer is subtracted. The first wave, which appears at ~0.5 μs, is caused by the ultrasonic wave that impinged directly on the diaphragm, as is evident from the fact that the temporal profile of the first wave is the same as that of the incident ultrasonic wave. At the immediate neighborhood of the rim of the diaphragm, the waveforms are deformed because shear waves are generated along the rim, which we will describe later. The amplitude at each position along the diameter appears to be almost uniform for the cases of z =250 and 150 mm, whereas it declines from the center to the rim for the case of $z = 50$

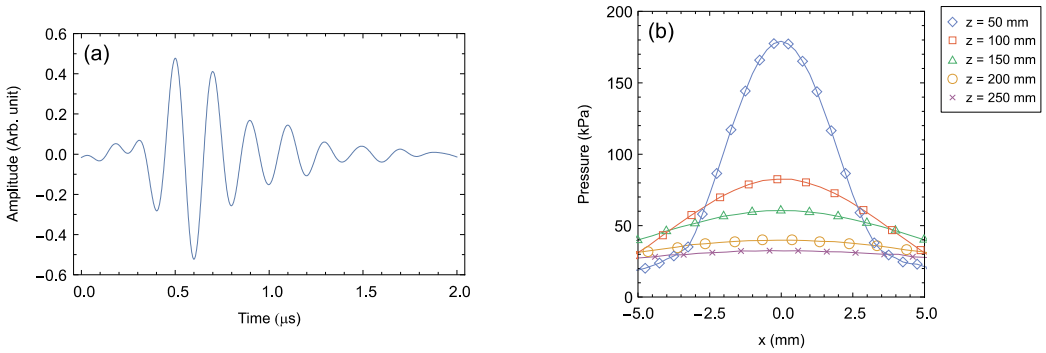

Fig. 2. (a) Waveform and (b) pressure distributions of an ultrasonic wave measured by a needle hydrophone.

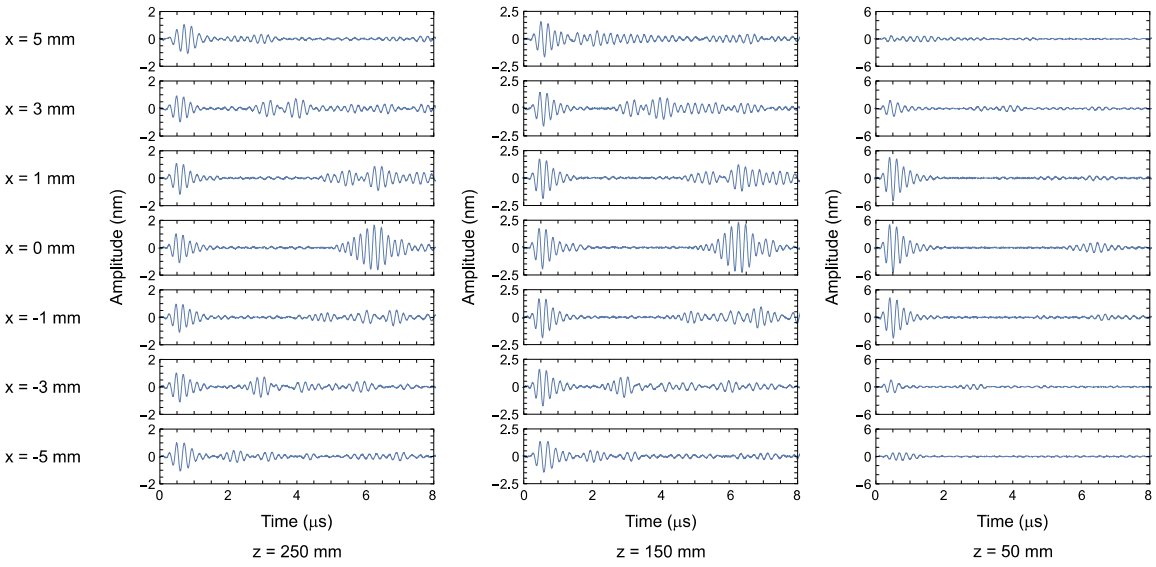

Fig. 3. Waveforms observed on the 10-mm-diameter diaphragm.

mm, reflecting the pressure profile of the incident ultrasonic wave at each distance. However, the amplitude at the center monotonically increases with decreasing distance in keeping with the pressure at the center of the pressure profile.

Following the first wave that coincides with the ultrasonic wave, the second wave, which is most clearly observable at the center of the diaphragm (x = 0 mm), appears with a time delay. The evaluation of the time at which the second wave was detected as a function of position along the diameter has shown that the time delay increases linearly as the center of the diaphragm is approached, implying that the second wave is a shear wave that propagates from the circumference. At the center, the second wave has the maximum amplitude with a well-defined shape, implying that constructive interference of shear waves takes place to build up the second wave. Notice that the amplitude increases as the distance decreases from z = 250 mm to z = 150 mm though the amplitude drops as the distance further decreases to z = 50 mm, consistent with a pressure change with distance at x = ±5.0 mm, as mentioned in Fig. 2(b).

Figure 4 shows the waveforms observed at the center of the diaphragms with different diameters. The amplitude of the second waves increases with decreasing diameter, whereas that of the first waves is independent on it. This diameter dependence of the second waves indicates that the amplitude is decided by the pressure level on the rim of the diaphragms rather than that at the center, which is corroborated by the fact that the pressure profiles, as shown in Fig. 2(b), more or less resemble a Lorentzian distribution, and consequently smaller diaphragms undergo higher pressures on the

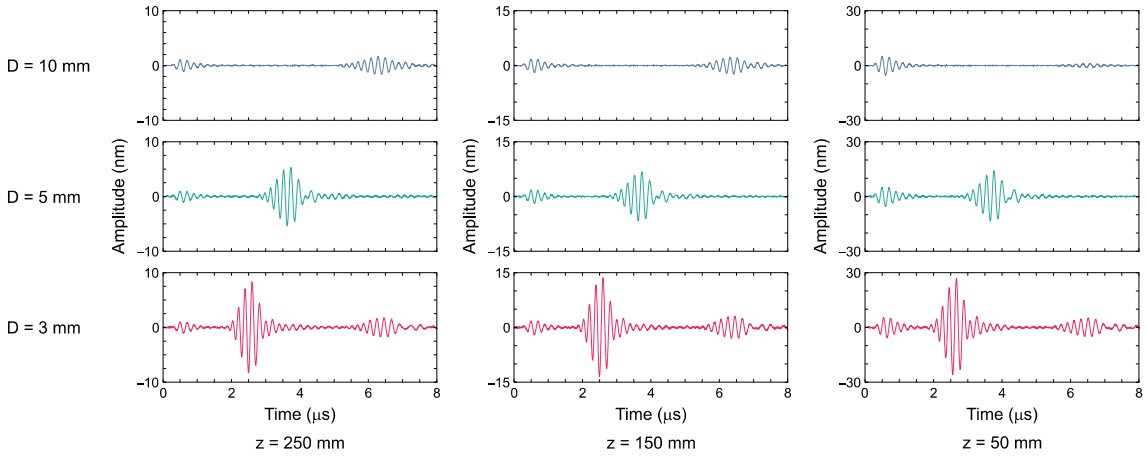

Fig. 4. Diameter dependence of the first and second waves.

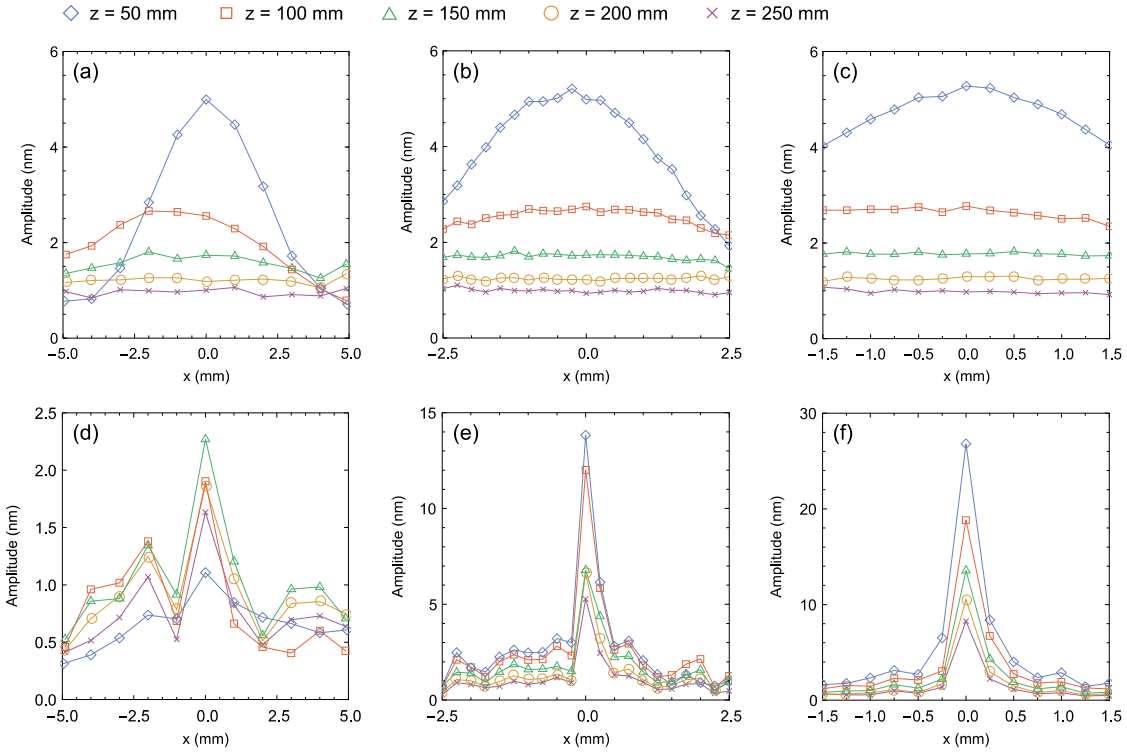

Fig. 5. Displacement profiles of diaphragms: (a) *D* = 10 mm, (b) *D* = 5 mm, and (c) *D* = 3 mm are caused by the first wave; (d) *D* = 10 mm, (e) *D* = 5 mm, and (f) *D* = 3 mm are caused by the second wave.

circumference. The dependence of the second wave on diameter is clearly seen even at z = 250 mm, where there is not much difference in pressure level between the center and the rim. This can be accounted for by attenuation of shear waves due to propagation. The time delay between the first and second waves is in proportion to the diameter. This again leads to the thought that the shear waves are emitted from the rim of the diaphragms, as well as the diameter dependence of the amplitude of the second waves. It is worth mentioning here that in the case of D = 3 mm, following the second wave at ~2 μs, a wave is present at ~6 μs. Obviously, this wave is composed of the shear waves that travel back to the center after reflection on the opposite point on the rim.

Figure 5 shows the displacement profiles of the diaphragms, corresponding to the maximum

amplitude observed at position along the diameter for the first and second waves. In the case of the first wave, the entire surface of the diaphragms appears to be shifted in proportion to the pressure caused by the incident ultrasonic wave, resulting in the similar shape as the pressure distribution shown in Fig. 2(b). From a comparison of the amplitude on the corresponding range along the diameter among the three diaphragms, it is evident that the amplitude of the first wave is independent on the diameter. In the displacement profiles for the second wave, on the other hand, a characteristic central peak with a narrow width is seen on each diaphragm, demonstrating that the second wave is formed by constructive interference of shear waves. This characteristic shape is further emphasized in smaller diaphragms. The amplitude of the central peaks depends on the pressure exerted on the rim of the diaphragms, as is evident from Fig. 2(b).

On the basis of these findings and arguments, we can best explain the generation mechanism of the second wave as follows. The diaphragm is initially displaced from its equilibrium position in proportion to the pressure caused by the incident ultrasonic wave, which we can observe as the first wave. The circumference of the diaphragm is clamped to the circular aperture on the substrate and becomes a geometrical discontinuity, so that strain is concentrated along the rim owing to a bending load caused by the displacement. This localized strain serves as ultrasonic sources arranged in a circle, exciting shear waves through the elastic relaxation of the strain. The emitted shear waves travel the equal path length toward the center of the diaphragm, at which all shear waves are added in phase to produce constructive interference. Hence, the second wave is observed at the center of the diaphragm, with a significantly large amplitude compared with that of the first wave.

As to the first wave, we did not clearly observe the dependence of the amplitude on the diameter of the diaphragms. If uniform static pressure is applied to the diaphragms, then the amplitude or the displacement depends on the diameter, and the shape of the surface eventually evolves into a quasi-semispherical shape at steady state. For our experiments, the diaphragms were exposed to the dynamic pressure caused by ultrasonic waves, in which case the amplitude is determined by the diaphragm's frequency response at the frequency of the incident ultrasonic wave. Natural frequencies of our diaphragms, which are proportional to d/r^2, where d and r are the thickness and diameter of the diaphragms, respectively [5], lie in the range of several hundred Hz. Although a decrease in diameter from 10 to 3 mm leads to an increase in natural frequency by a factor of 10, the frequency of the ultrasonic wave (5 MHz) is likely to be out of the sensitive range of the diaphragm's frequency response since the deviation between those frequencies is still three orders of magnitude. In addition, water will lower the natural frequency. It follows from these considerations that the first wave is independent on the diameter, and the amplitude is decided by the pressure level of the incident ultrasonic wave, provided that the frequency of the ultrasonic wave is far away from the natural frequency of the diaphragms.

In Fig. 6, the amplitudes of the first and second waves are plotted as a function of pressure at the center and rim of the diaphragms, respectively. We calculated the sensitivities as the slope of the best fitting lines to the measurement data of amplitude and pressure, using the least-squares method. The sensitivity for the first wave is found to be 0.034 ± 0.001 nm/kPa regardless of the diameters. In the case of the second wave, the sensitivity increases with decreasing diameter, found to be 0.06, 0.17, and 0.26 nm/kPa for D = 10, 5, and 3 mm, respectively. Compared with the results obtained with the first wave, the sensitivity is improved by a factor of 7 for the 3-mm-diameter diaphragm, highlighting the potential to improve the sensitivity of an optical ultrasonic sensor without having to reduce the thickness of the diaphragm. The improved sensitivities for the stainless steel diaphragms are still lower than those for silver, silica, and graphene diaphragms reported in Refs. 6-8 by two orders of magnitude. Nevertheless, it should be pointed out that the improvement method based on the second wave, or shear waves, is of particular importance in the development of sensitive and robust optical ultrasonic sensors for USVs because these sensors cannot always take advantage of thin diaphragms of sub-micron thicknesses and novel materials available in the literature in order to improve the sensitivity for the reasons stated in the introduction.

The amplitudes of the first and second waves show a good linear response to pressure although deviation of the measurement data from the lines is slightly large in the case of the second wave. This may be attributed to the alignment accuracy of the measurement laser beam since the second wave results from interference of shear waves at the center of the diaphragms (see Fig. 5). Also, the symmetry and uniformity of the diaphragms have an influence on the generation of the second wave.

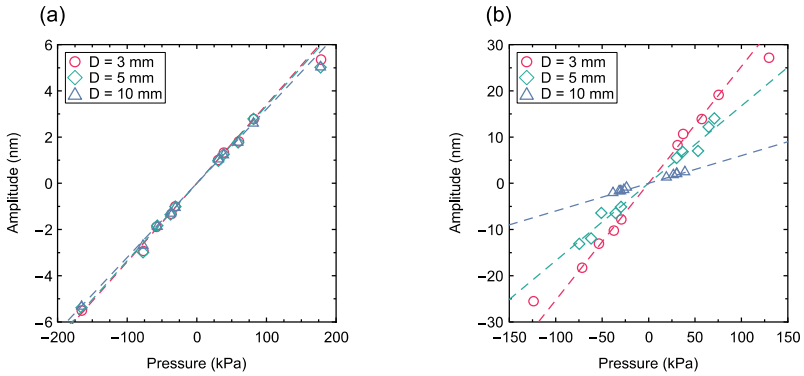

Fig. 6. Amplitudes of (a) the first and (b) second waves as a function of pressure.

The linearity and repeatability of the amplitudes will be affected by all of these factors and should be investigated in the next step experiments.

4. Conclusion

We have experimentally investigated shear waves induced on stainless steel diaphragms in order to understand the generation mechanism of the second wave and explored the possible use of the shear waves for improvement of the sensitivity of an optical ultrasonic sensor used for under-sodium viewers. The generation mechanism is summarized below. The incident ultrasonic wave initially causes a displacement of the diaphragm, which is observed as the first wave. The shear waves are then excited through the elastic relaxation of the strain that is concentrated along the rim of the diaphragm owing to a bending load caused by the displacement. The shear waves propagate over the equal path length and meet in phase at the center of the diaphragm; therefore, we observe constructive interference of these shear waves as the second wave with a significantly large amplitude compared with that of the first wave. The experimental results have demonstrated that the sensitivity can be improved by using the second wave. We have achieved the sensitivity of 0.26 nm/kPa for the 3-mm-diameter and 5-μm-thick diaphragm, which is approximately 7 times as high as the sensitivity obtained with the first wave. Also, the amplitude of the second wave increases with decreasing diameter, allowing us to improve the sensitivity further by reducing the diameter instead of reducing the thickness of the diaphragm.

References

[1] H. Karasawa, M. Izumi, T. Suzuki, S. Nagai, M. Tamura, and S. Fujimori: "Development of under-sodium three-dimensional visual inspection technique using matrix-arrayed ultrasonic transducer", J. Nucl. Sci. Technol., Vol. 37, No. 9, pp. 769-779 (2000).

[2] A. Tagawa and T. Yamashita: "Development of real time sensor for under sodium viewer", Proceedings of the 19th International Conference on Nuclear Engineering, Makuhari, Japan, May 16-19, ICONE19-43187 (2011).

[3] M. Takeishi, K. Shibaike, T. Ito, H. Yanagida, M. Tamura, and S. Fujimori: "Development of multiple ultrasonic transducer by optical method for under sodium viewer", Proceedings of the 6th International Conference on Nuclear Engineering, San Diego, USA, May 10-15, ICONE6-6115 (1998).

[4] K. Aizawa, Y. Chikazawa, K. Ara, M. Yui, Y. Uemoto, M. Kurokawa, and T. Hiramatsu: "Development of under sodium viewer for next generation sodium-cooled fast reactors", Proceedings of the International Conference on Fast Reactors and Related Fuel Cycles; Next Generation Nuclear Systems for Sustainable Development, Yekaterinburg, Russia, June 26-29, IAEA-CN-245-267 (2017).

[5] M. D. Giovanni: "Flat and corrugated diaphragm design handbook", CRC Press, New York (1982).

[6] F. Guo, T. Fink, M. Han, L. Koester, J. Turner, and J. Huang: "High-sensitivity, high-frequency extrinsic Fabry-Perot interferometric fiber-tip sensor based on a thin silver diaphragm", Opt. Lett., Vol. 37, No. 9, pp.

1505-1507 (2012).
[7] D. Donlagic and E. Cibula: "All-fiber high-sensitivity pressure sensor with SiO_2 diaphragm", Opt. Lett., Vol. 30, No. 16, pp. 2071-2073 (2005).
[8] J. Ma, W. Jin, H. L. Ho, and J. Y. Dai: "High-sensitivity fiber-tip pressure sensor with graphene diaphragm", Opt. Lett., Vol. 37, No. 13, pp. 2493-2495 (2012).
[9] K. Saruta, T. Yamaguchi, and M. Ueda: "Effects of metallic diaphragms on sensitivity characteristics of an optical ultrasonic sensor and reduction of interrogation time based on wavelength division multiplexing for under-sodium visual inspection", E-Journal of Advanced Maintenance, Vol. 7, No. 4, http://www.jsm.or.jp/ejam/Vol.7No.4/NT/NT75/75.html.